Particle Acceleration in Pulsed Power Driven Magnetic Reconnection

Jack W. D. Halliday (jack.halliday12@imperial.ac.uk)

Imperial College: J. D. Hare, L. G. Suttle, S. V. Lebedev, S. N. Bland, E. R. Tubman, D. R. Russell, T. A. Clayson, F. Suzuki-Vidal

Cornell University & Lebedev Institute: S. A. Pikuz, and T. A. Shelkovenko.

Imperial College London

MAGPIE

Talk Outline

- MAGPIE reconnection platform
- Diagnosing energetic particles
- Measurements of accelerated electrons

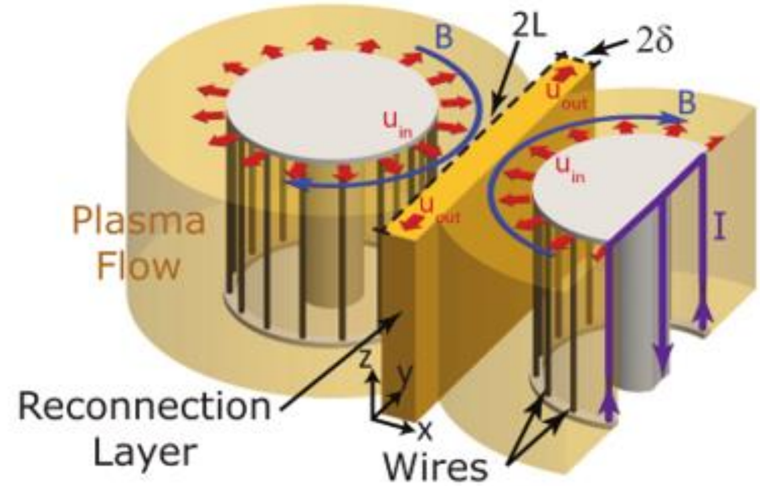

[L. G. Suttle *et al.* – PRL 2016; PoP 2018]

[J. D. Hare *et al.* – PRL 2017; PoP 2017; PoP 2018]

MAGPIE Pulsed-Power Generator

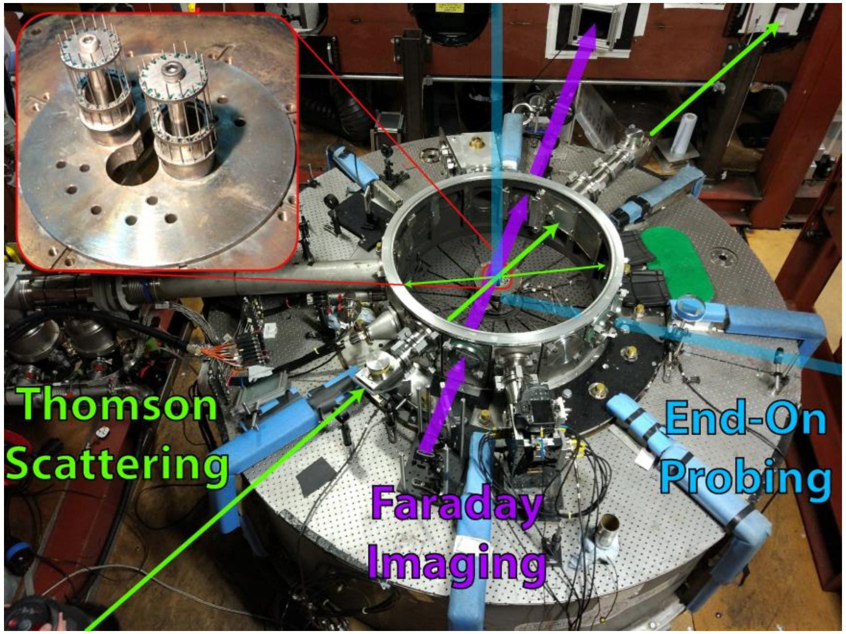

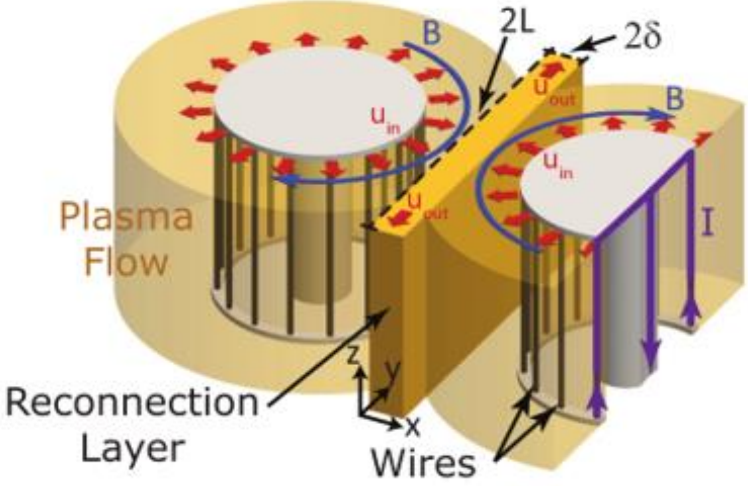

Sub-Alfvénic Regime

T_{drive}	L	B_{in}	β_{ram}	$\beta_{thermal}$	S
500 ns	~10 mm	3 T	~ 1	~ 1	~ 100

Magnetic Reconnection Platform

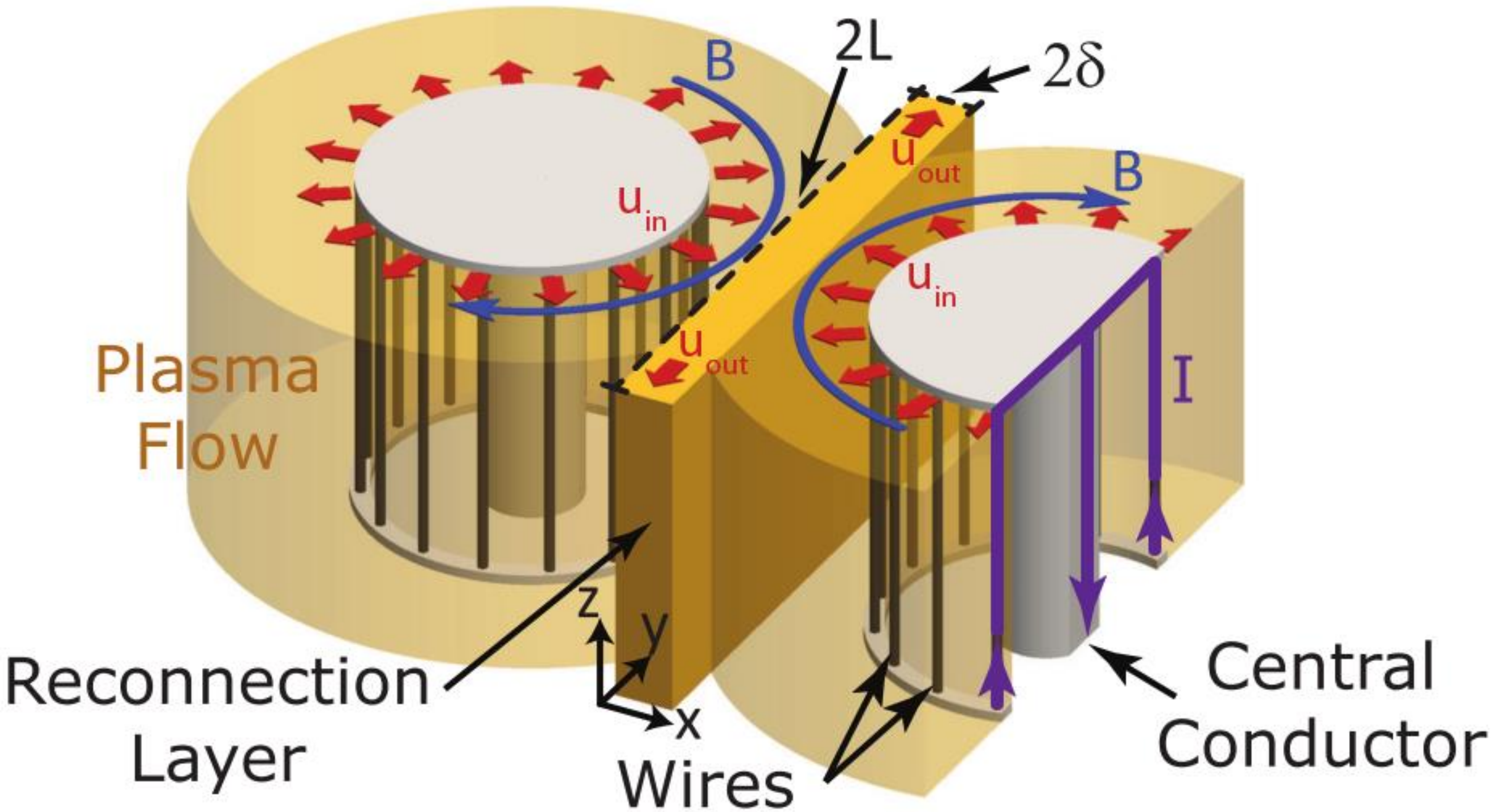

Magnetic Reconnection Platform

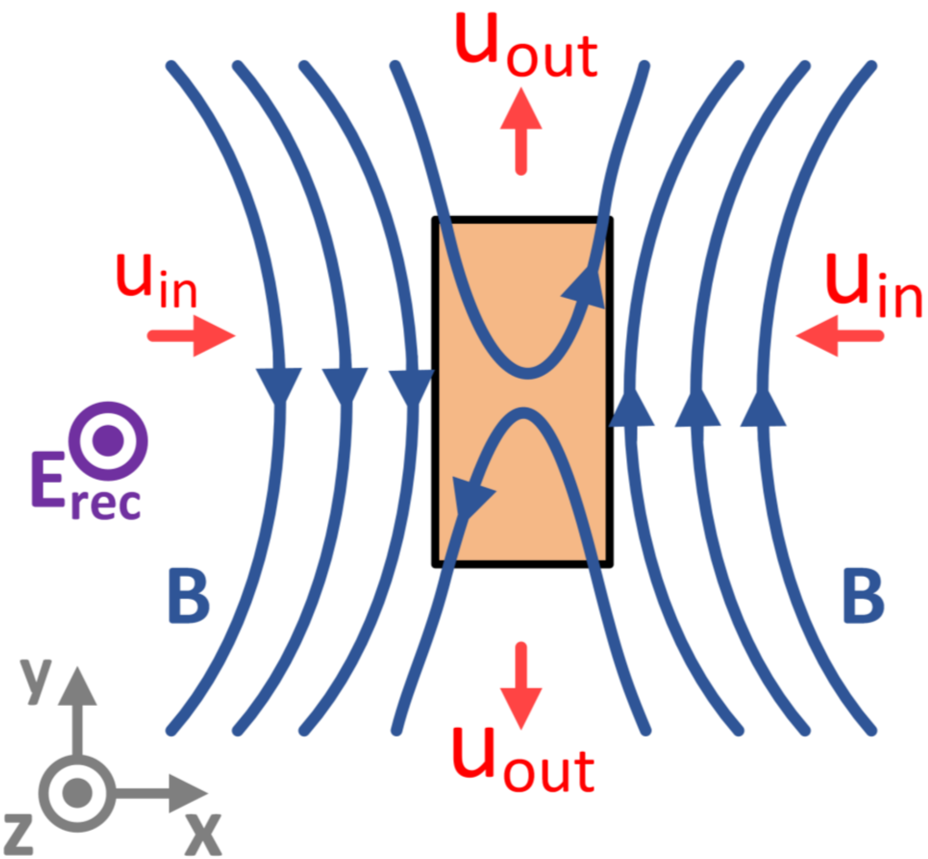

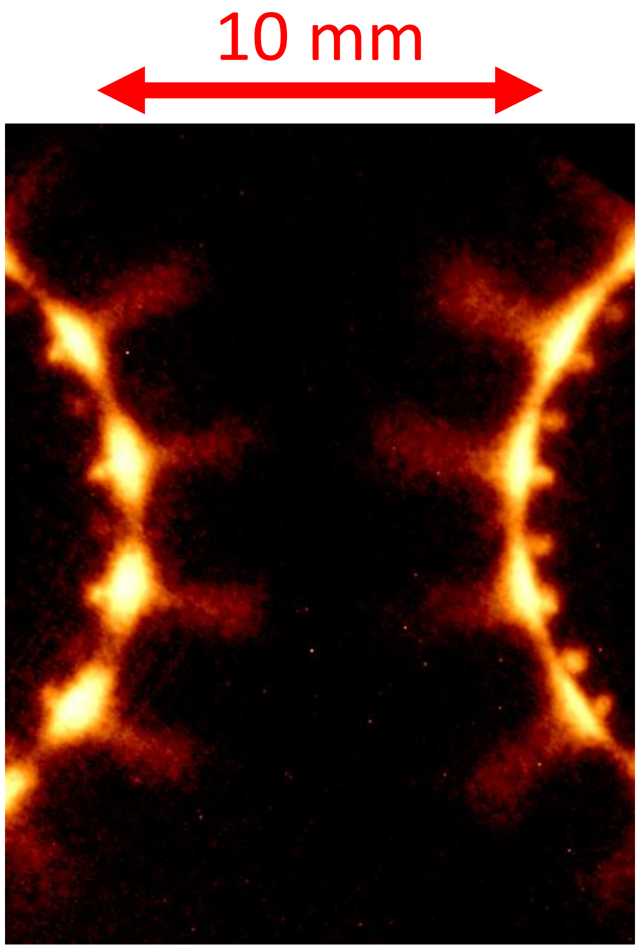

Direct Electron Acceleration

End-On View (X-Y Plane)	Side-On View (X-Z Plane)

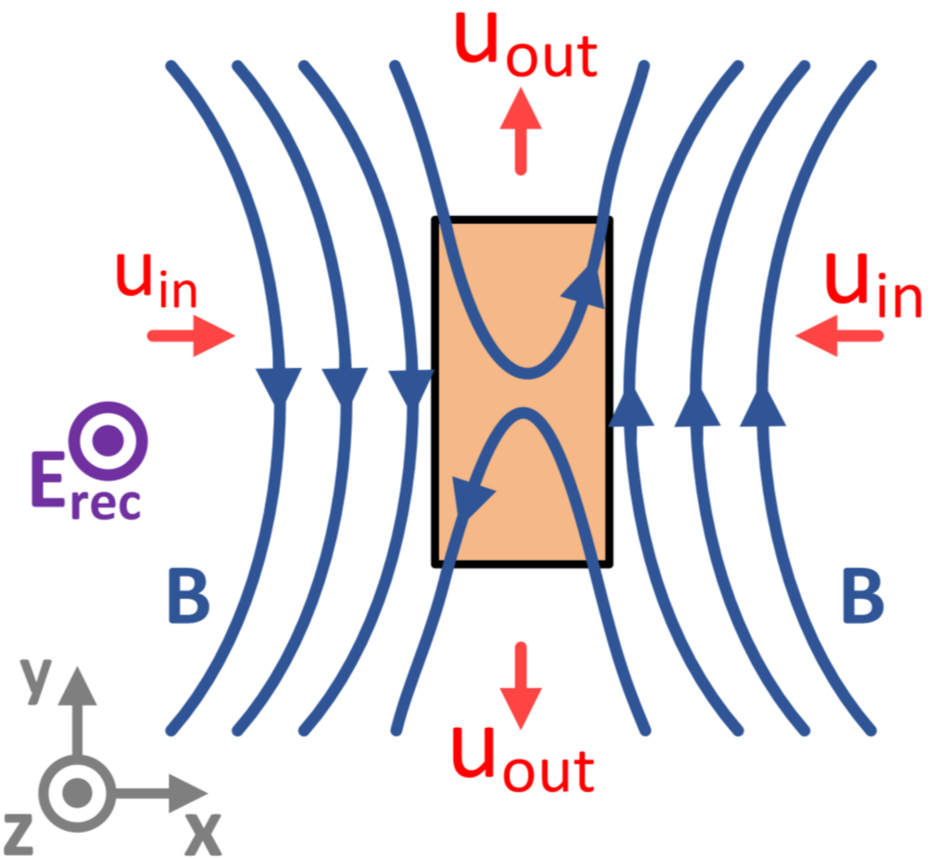

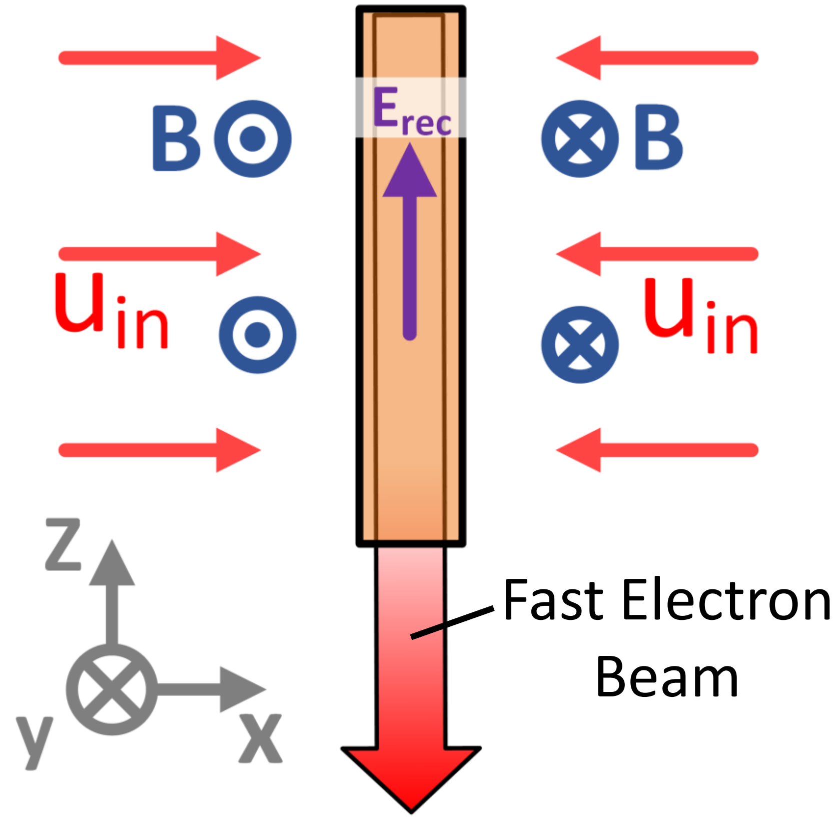

Reconnecting Electric Field

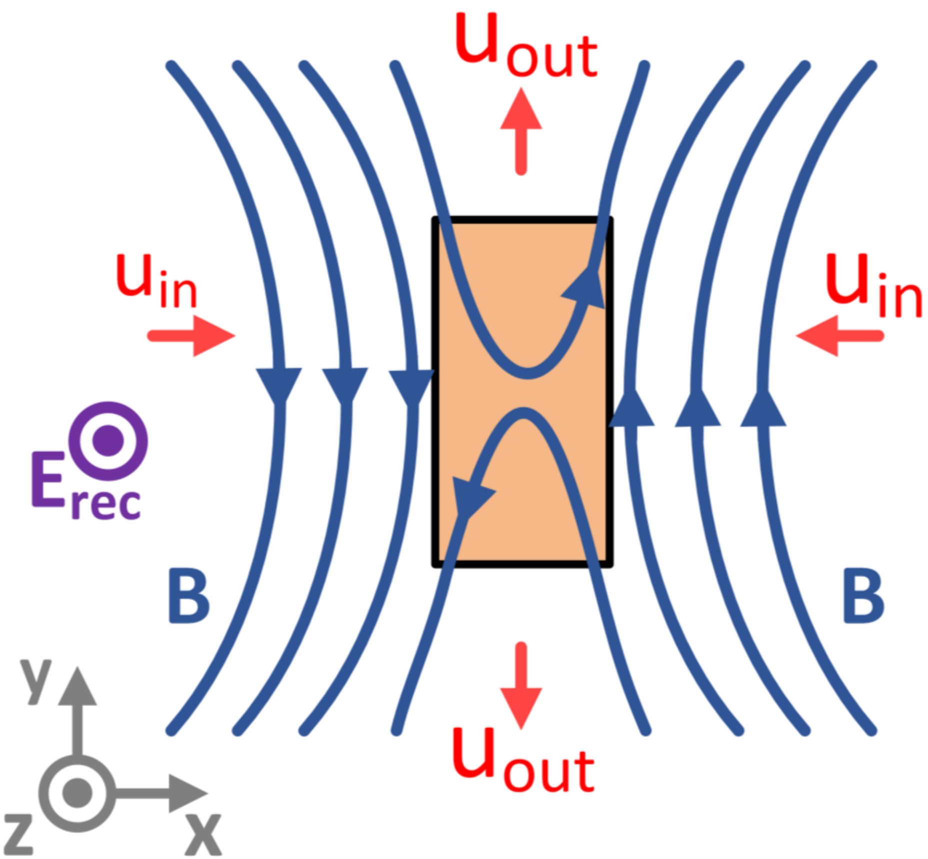

Parameter	Value	Diagnostic
u_{in}	50 km/s	Thomson Scattering
B_{in}	3 T	Faraday Rotation
L_z	16 mm	Interferometry

$$\mathbf{E} = -\mathbf{u} \times \mathbf{B} + \eta\mathbf{j}$$

$$E_{rec} = u_{in}B_{in} = 150\ \mathrm{kV/m}$$

$$\int \mathbf{F}.\,d\mathbf{l} \sim eE_{rec}L_z = \mathbf{2.4\ keV}$$

Diagnosing Accelerated Electrons

End-On View (X-Y Plane)	Side-On View (X-Z Plane)

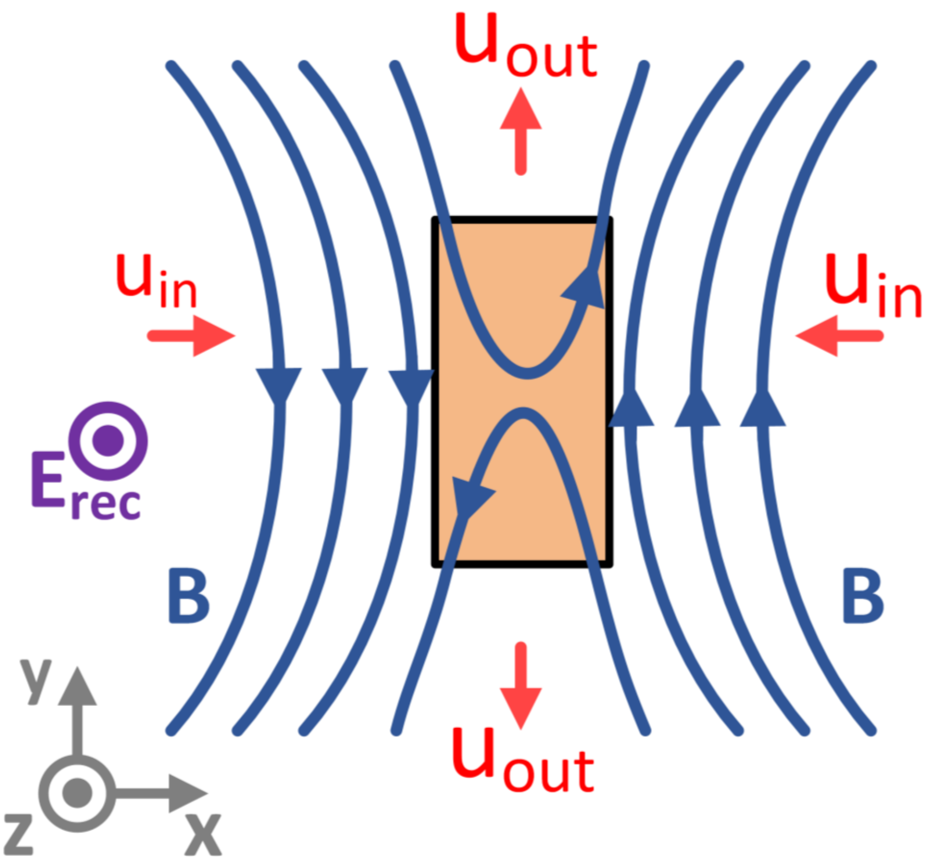

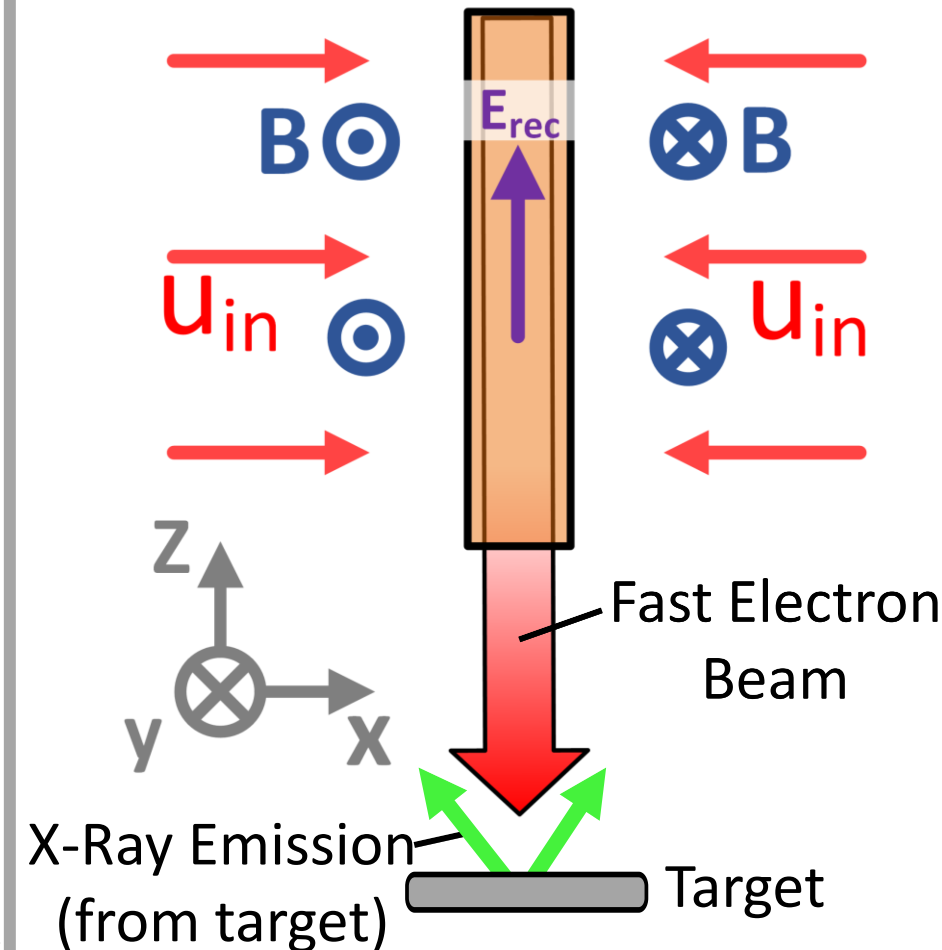

X-Ray Imaging and Spectroscopy

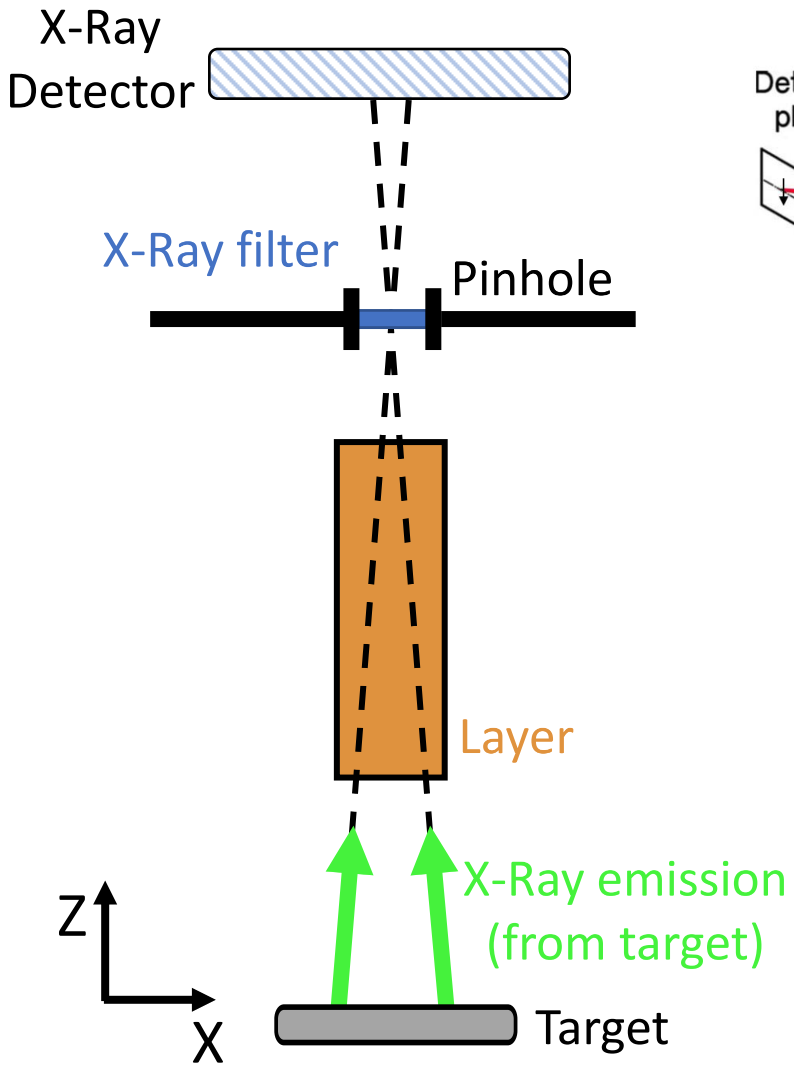

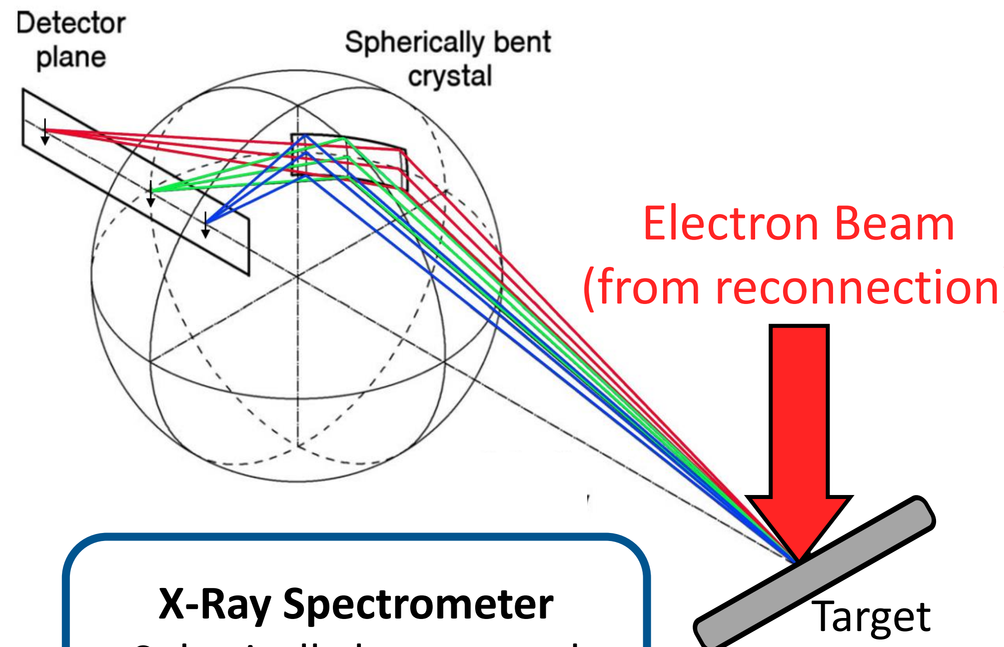

X-Ray Spectrometer
Spherically bent crystal
(Mica, R=186mm)

(Figure adapted from S. A. Pikuz et al. 2008. Rev Sci Instr. 79, 013106)

Time Integrated Pinhole Imaging

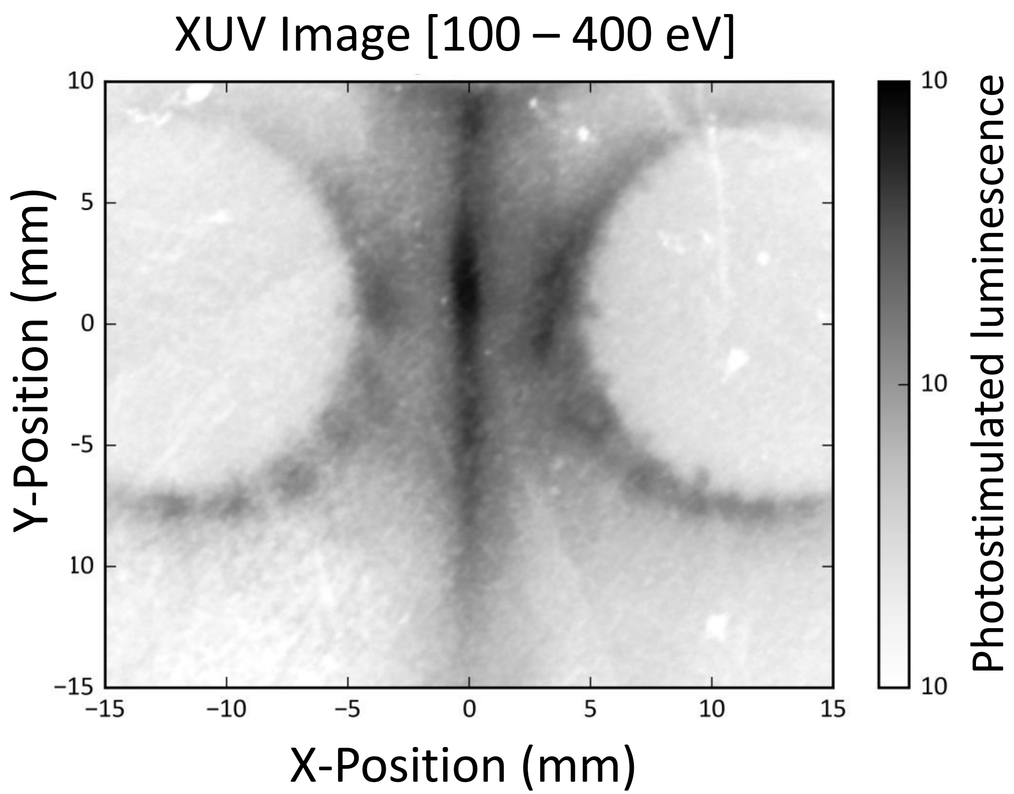

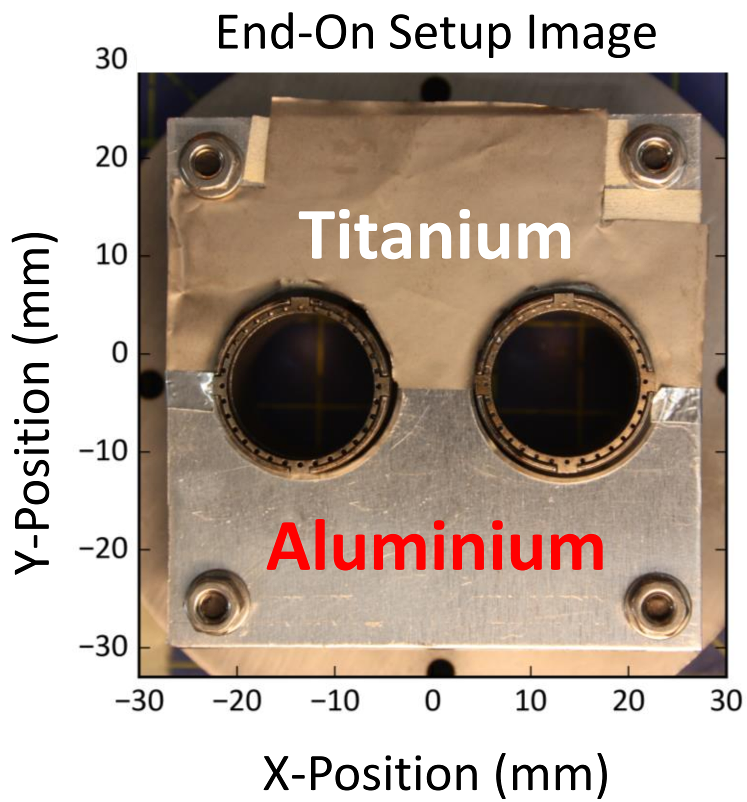

Thomson Scattering ⇒ $T_e \leq 100$ eV

Time Integrated Pinhole Imaging

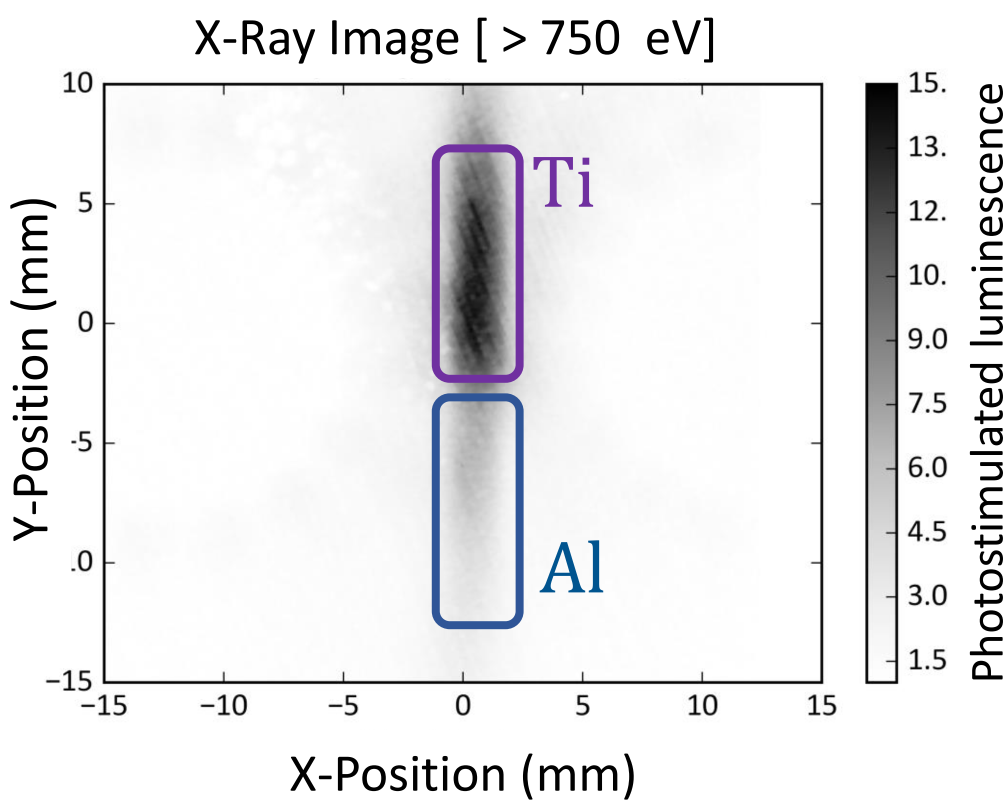

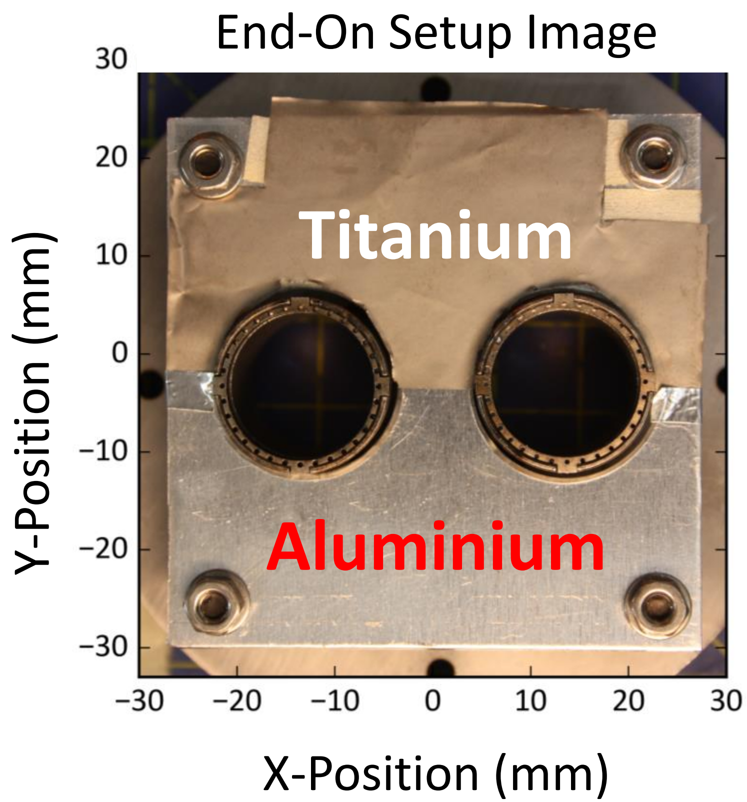

Thomson Scattering ⇒ $T_e \lesssim 100$ eV

Time Resolved X-Ray Imaging Data

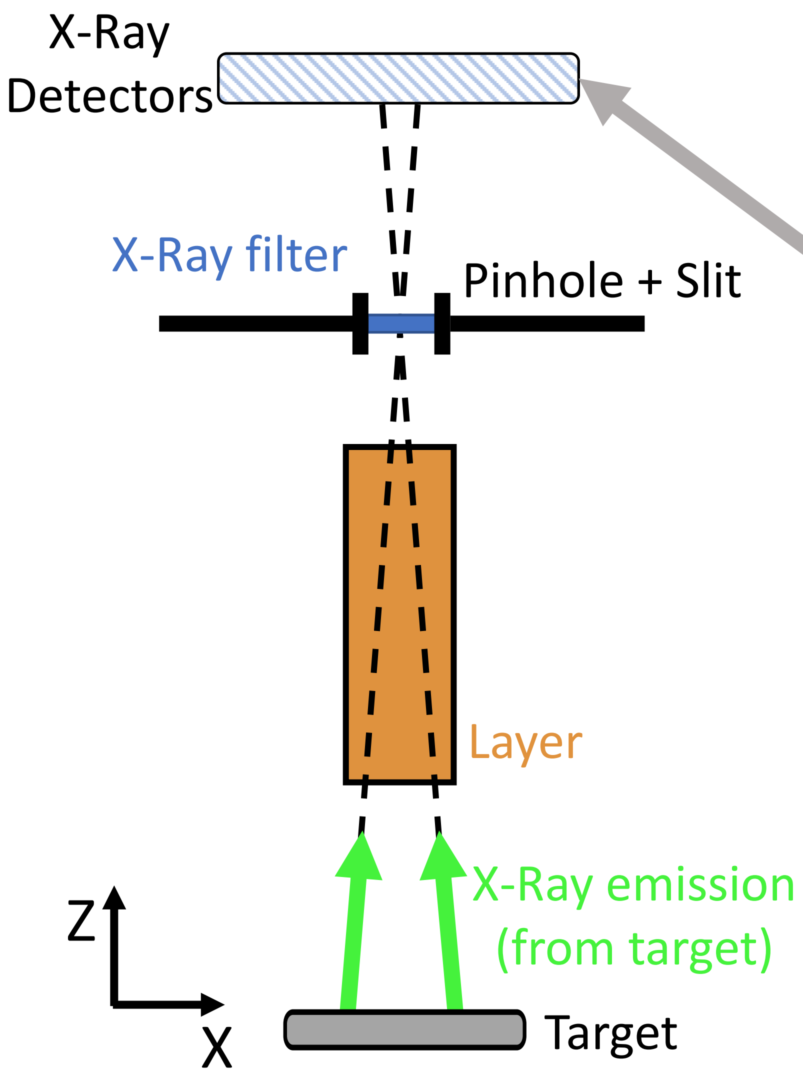

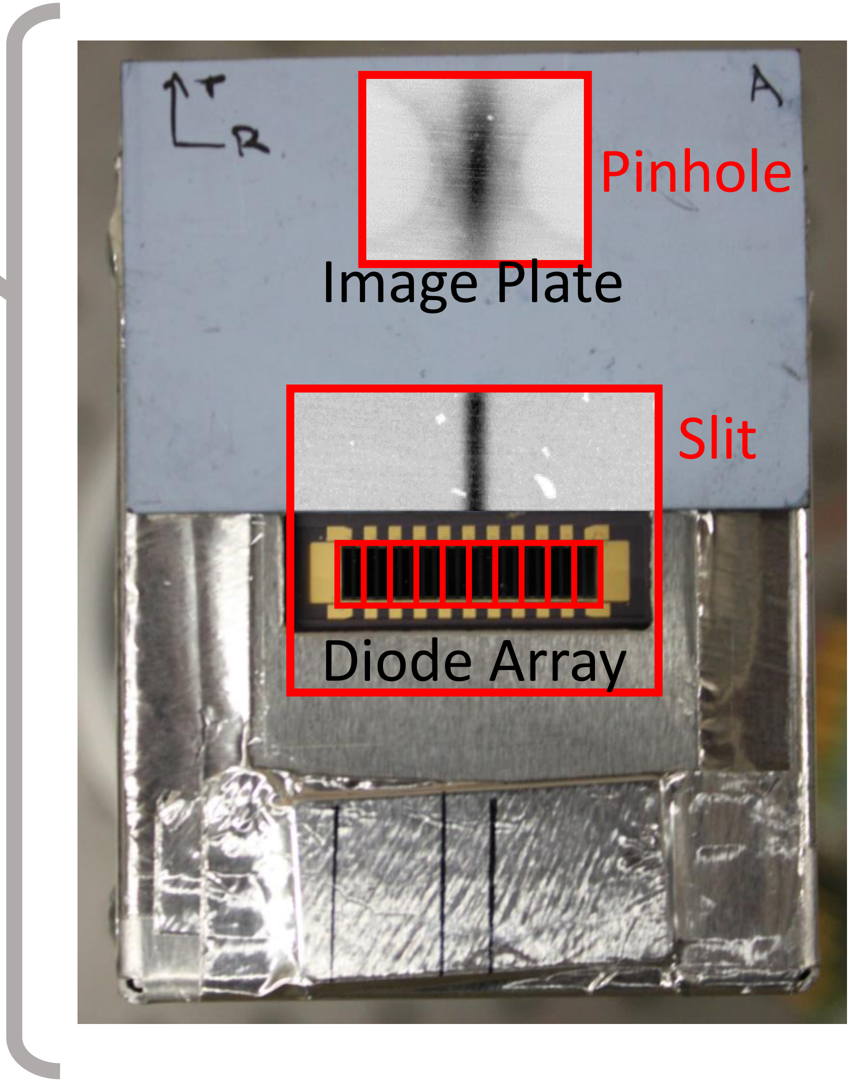

Time Resolved X-Ray Imaging Data

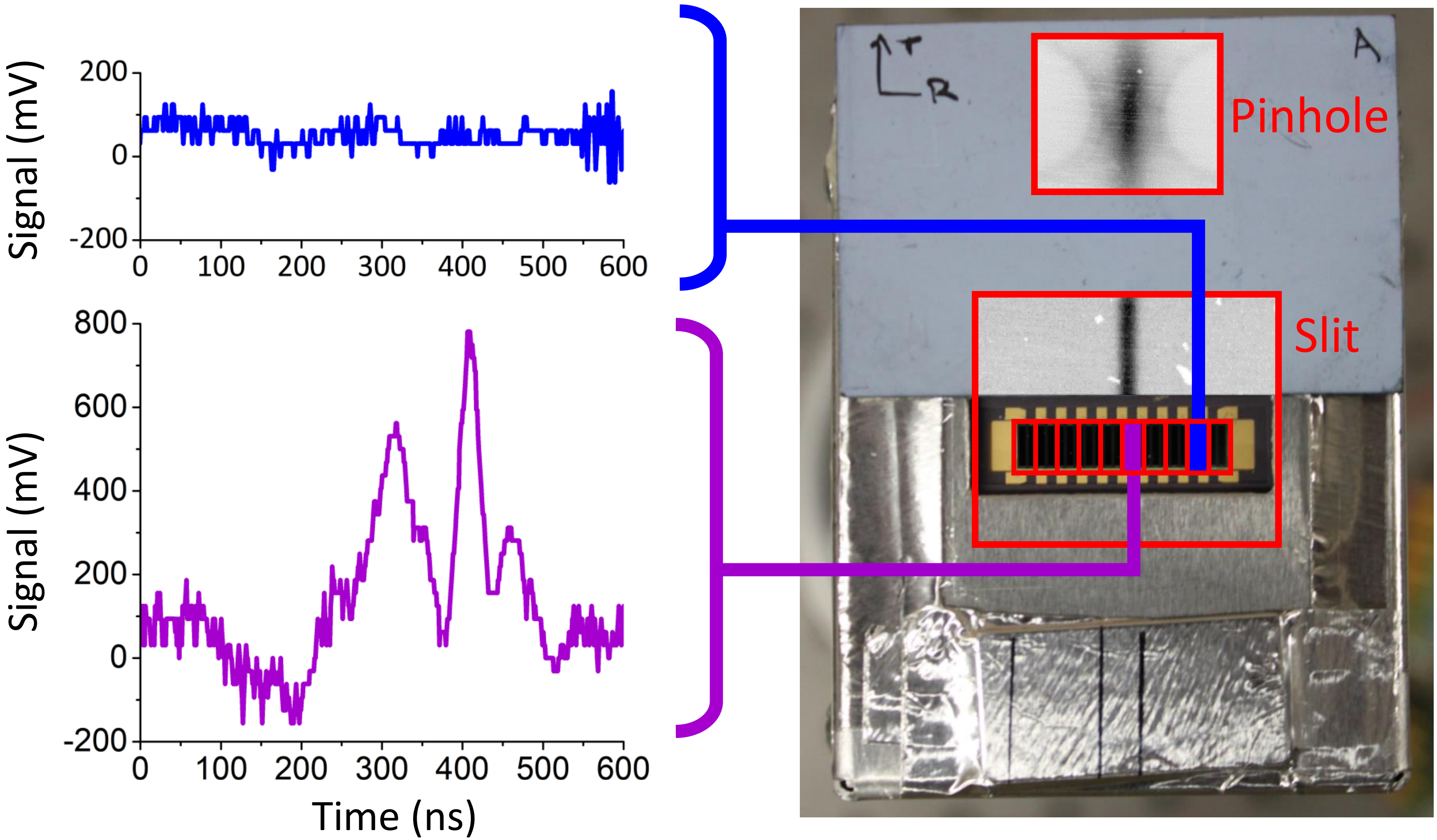

Time Resolved X-Ray Imaging Data

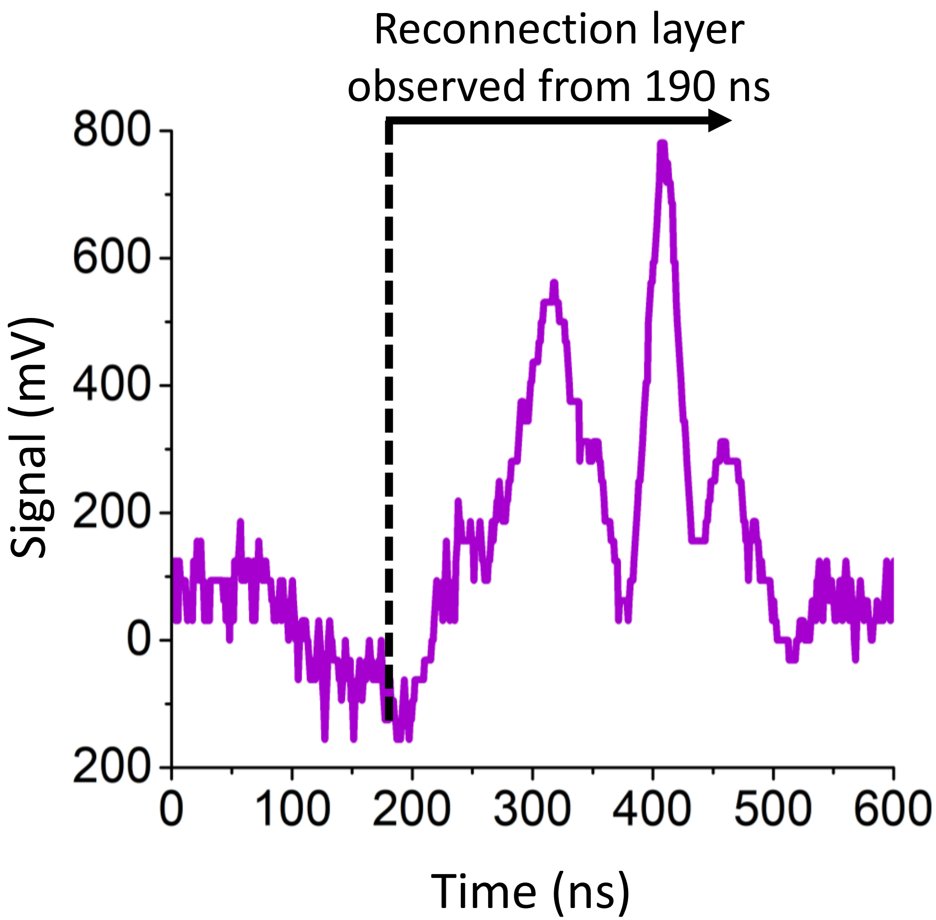

End-On Electron Density (t = 190 ns)

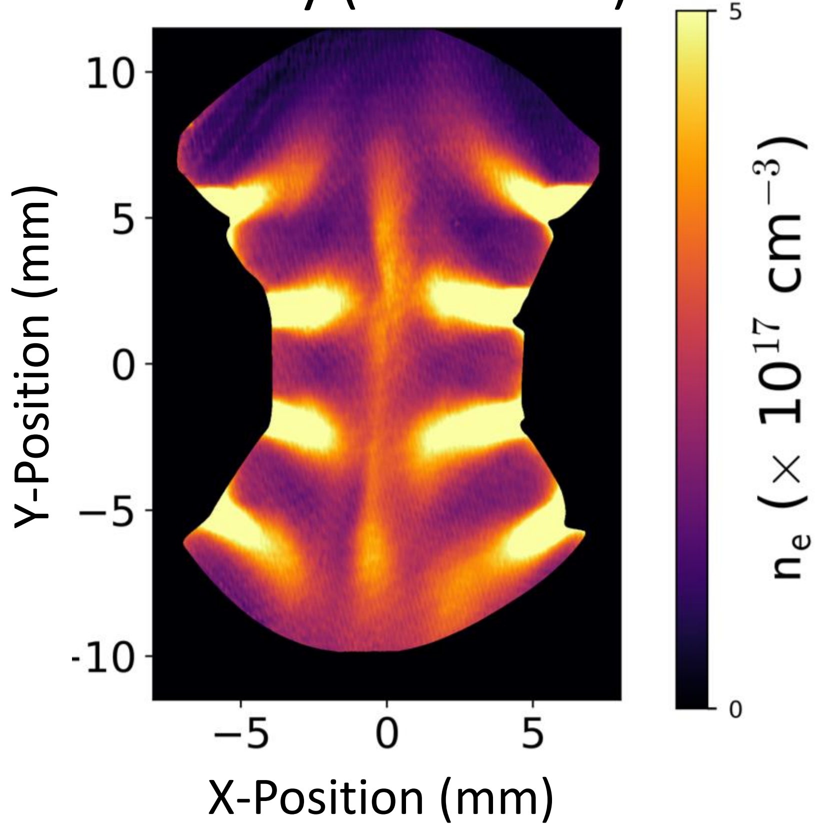

Time Resolved X-Ray Imaging Data

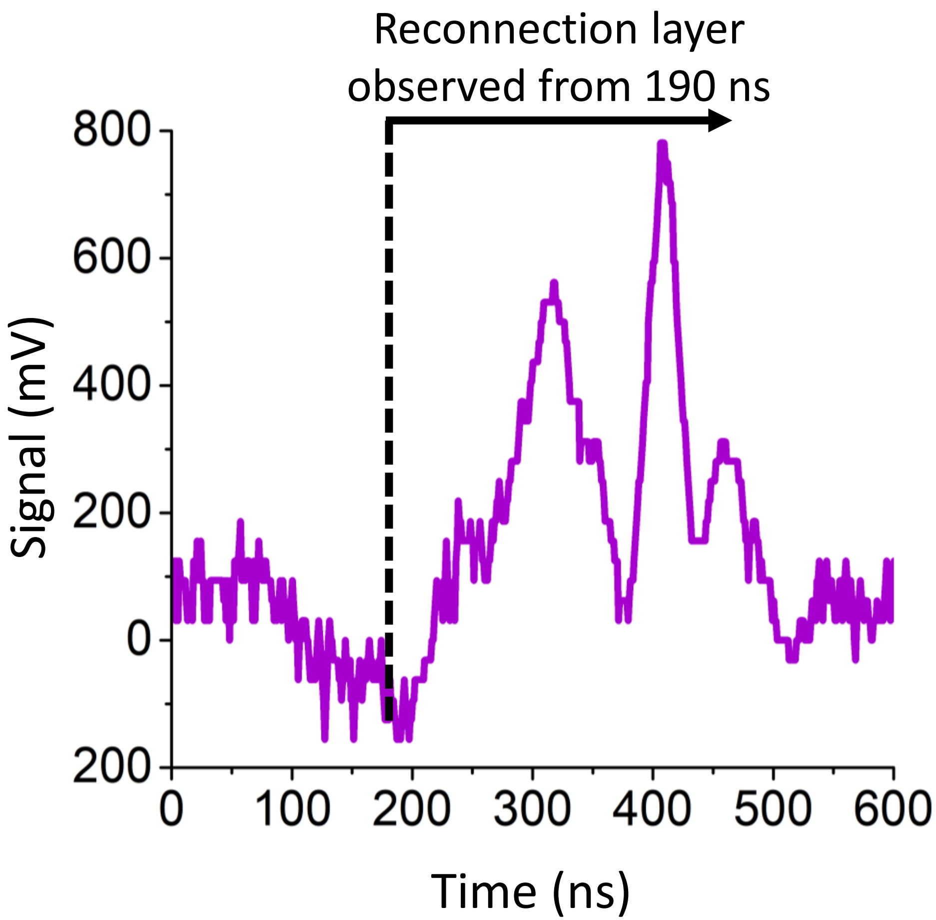

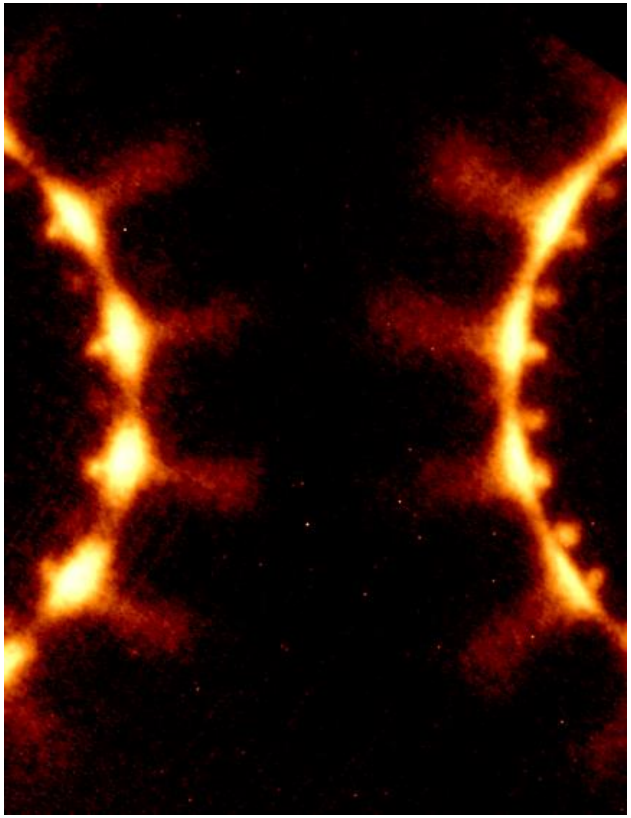

X-Ray Spectroscopy Data

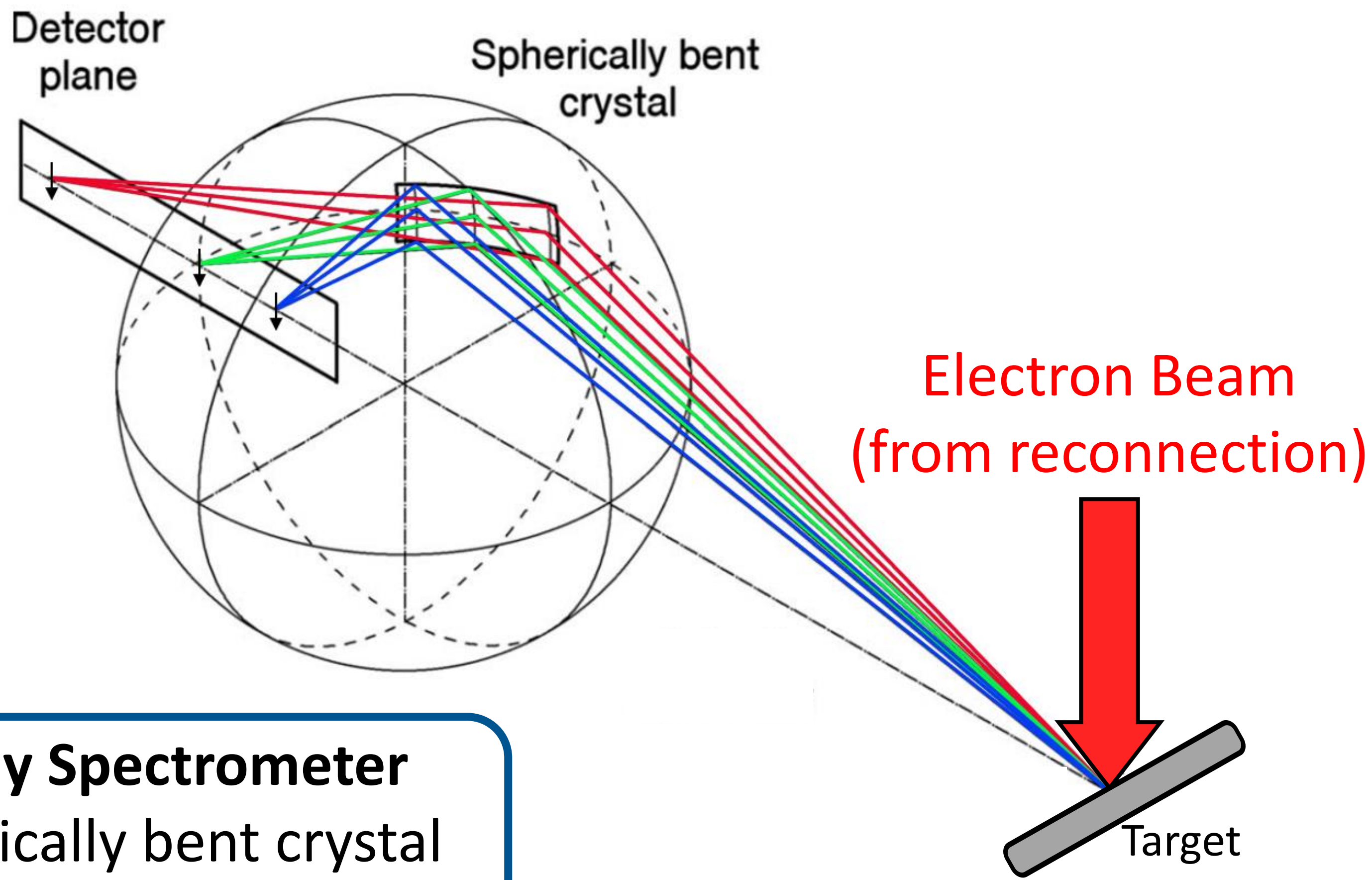

X-Ray Spectrometer
Spherically bent crystal
(Mica, R=186mm)

(Figure adapted from S. A. Pikuz et al. 2008. Rev Sci Instr. 79, 013106)

Time Integrated X-Ray Spectra

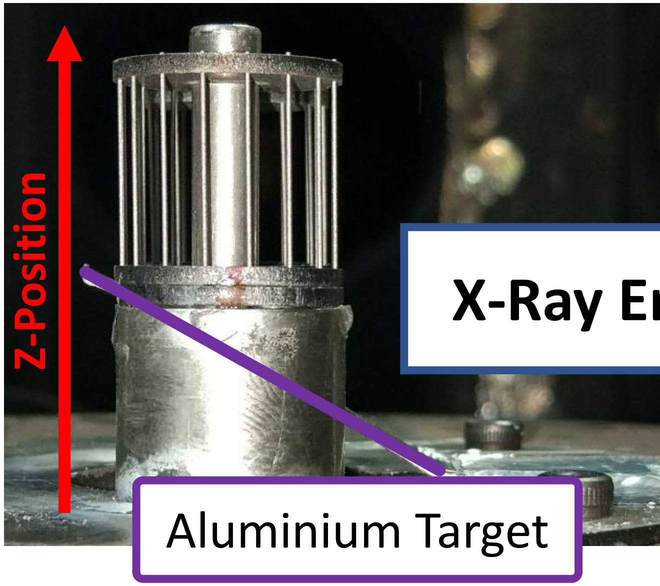

X-Ray Emission (from target)

Spherically Bent Crystal Spectrometer

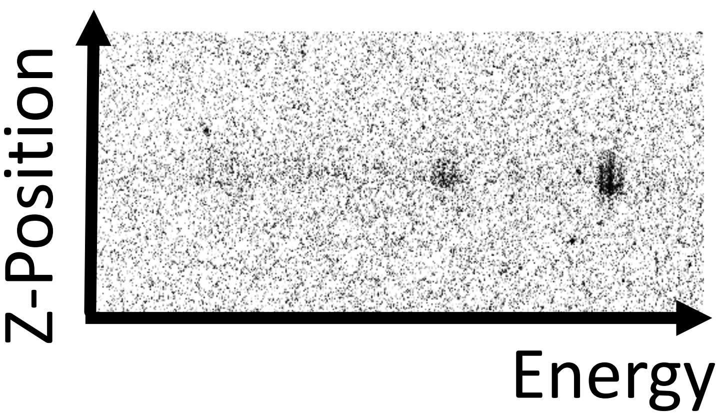

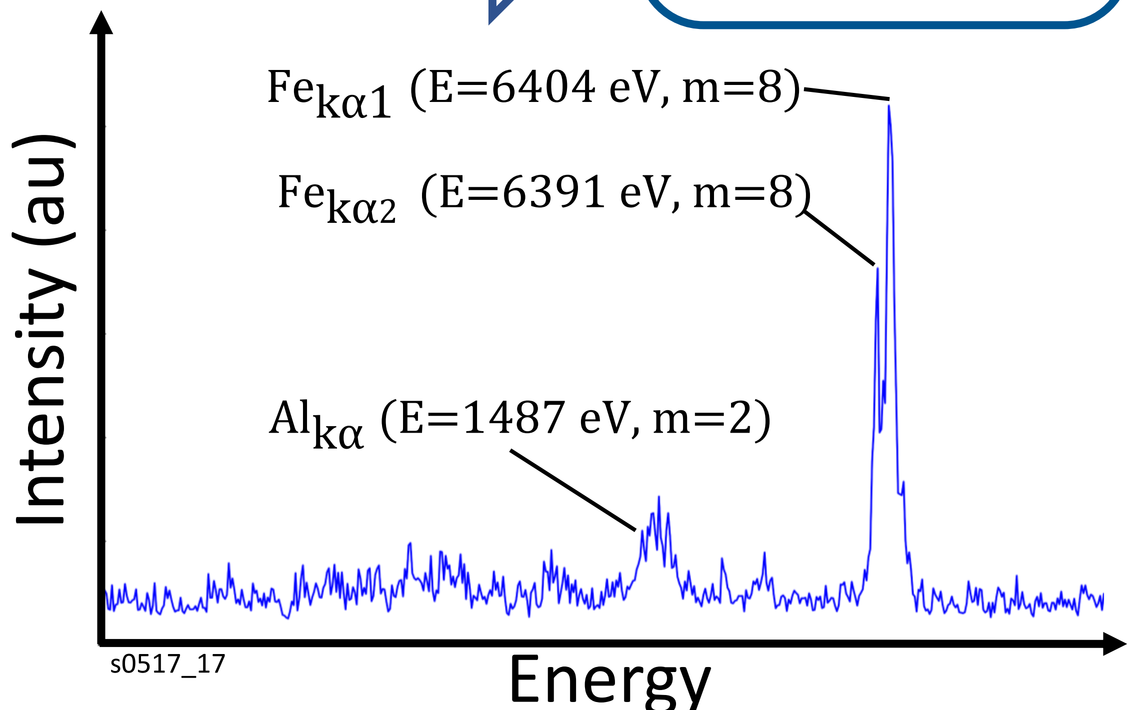

Conclusions

X-Ray Image [750 – 1500 eV]

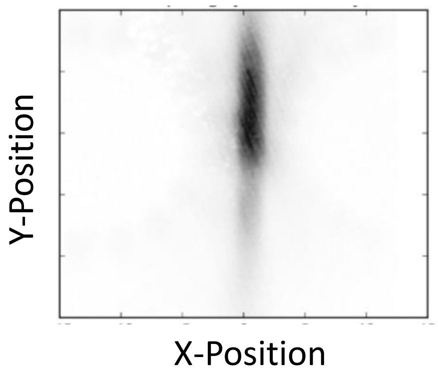

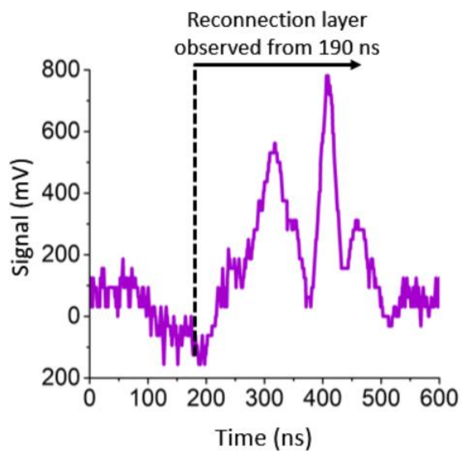

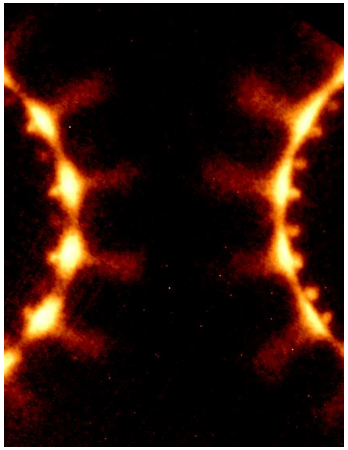

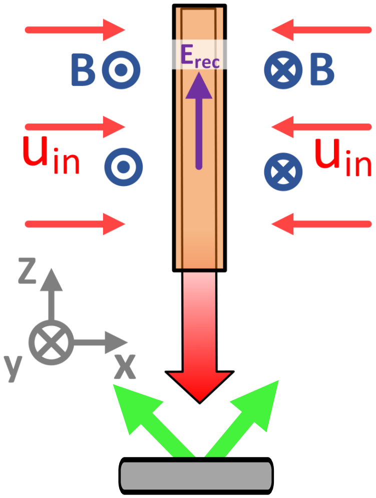

- Reconnection layer accelerates electrons to energies over 2 keV
- Consistent with acceleration by the reconnecting electric field
- Acceleration bursty ⇒ non steady-state / instabilities?

[L. G. Suttle *et al.* – PRL 2016; PoP 2018]
[J. D. Hare *et al.* – PRL 2017; PoP 2017; PoP 2018]

Plasma Parameters

Parameter		Carbon Flow	Carbon Layer
Electron density (cm^{-3})	n_e	3×10^{17}	6×10^{17}
Effective charge	$\bar{Z}$	4	6
Electron temperature (eV)	T_e	15	100
Ion temperature (eV)	T_i	50	600
Magnetic field (T)	B_y	3	…
Layer half-length (mm)	$L = R_C/2$	…	7
Layer half-thickness (mm)	δ	…	0.6
Ion skin depth (mm)	c/ω_{pi}	0.71	0.41
Ion-ion mean free path (mm)	$\lambda_{i,i}$	4×10^{-2}	3×10^{-3}

Parameter		Carbon Flow	Carbon Layer
Inflow (outflow) velocity (km/s)	$V_x (V_y)$	50	(130)
Alfvén speed (km/s)	V_A	70	…
Sound speed (km/s)	C_S	30	85
Fast-magnetosonic speed (km/s)	V_{FMS}	75	…
Ion-electron cooling time (ns)	$\tau^E_{e/i}$	30	140
Radiative cooling time (ns)	τ_{rad}	100	600
Thermal beta	β_{th}	0.4	…
Dynamic beta	β_{dyn}	1	…
Lundquist number	S	…	120
Two-fluid effects	L/d_i	…	18

Thermal Electrons: $\lambda_{ei} \sim 6 \times 10^{-3}\,\text{cm}$

2 keV Electrons : $\lambda_{ei} \sim 2.2\ \text{cm}$

Diagnosing Plasma Flows

Interferometry	Thomson scattering	Faraday-Rotation Imaging
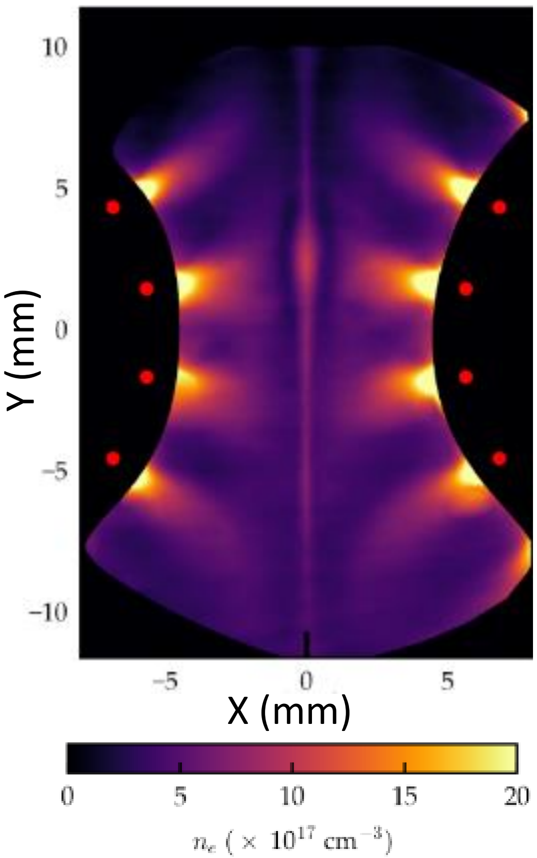	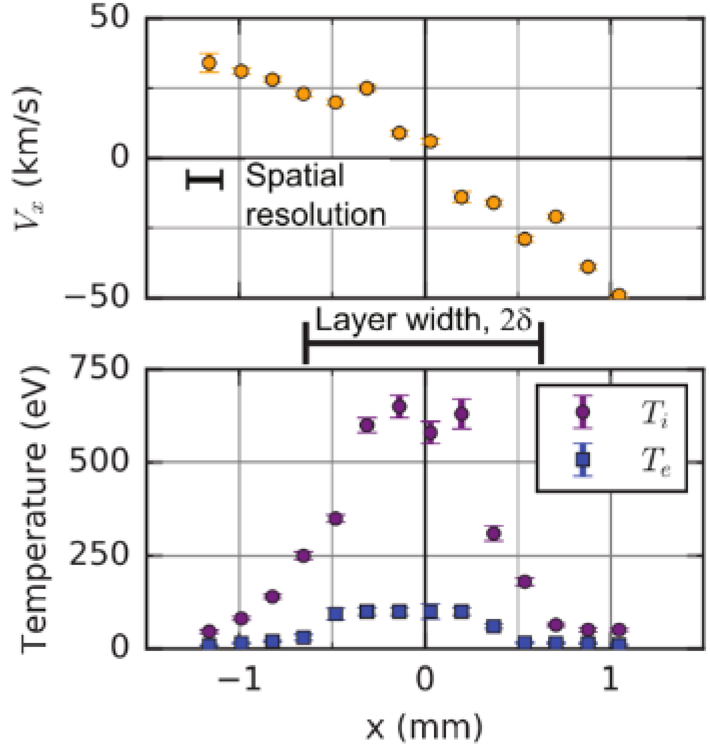	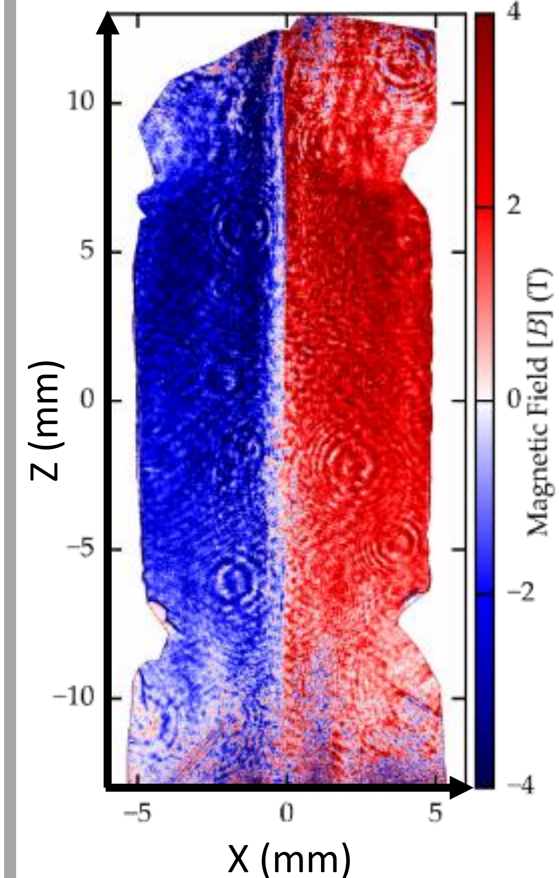

Diagnosing Plasma Flows

End-On View (X-Y Plane)

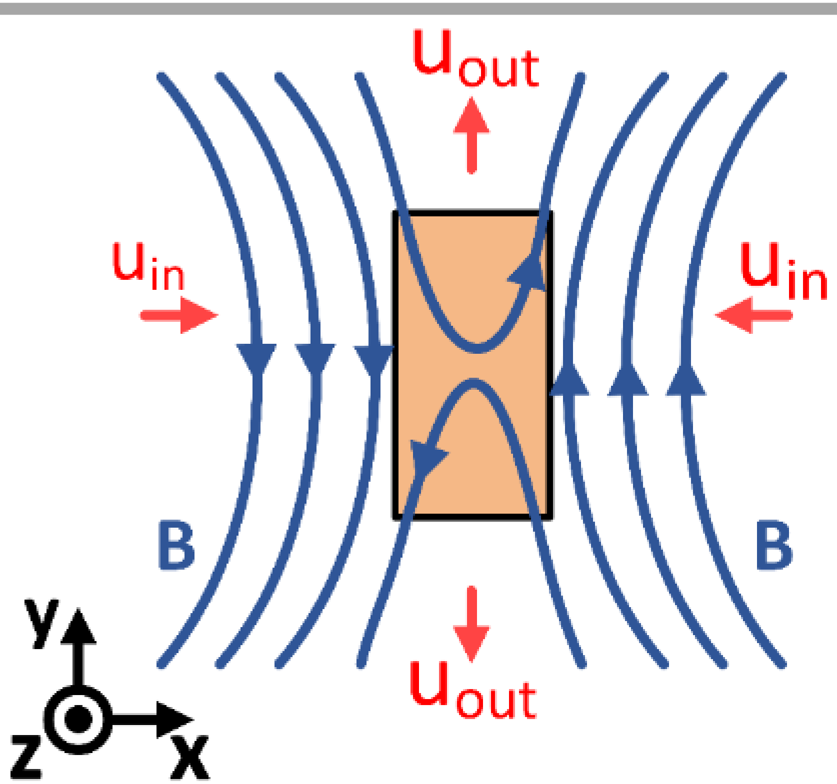

Interferometry ($\mathbf{n_e L}$)

Thomson Scattering ($\mathbf{u_x}$, $\mathbf{u_y}$, $\mathbf{T_e}$, $\mathbf{T_i}$)

Side-On View (X-Z Plane)

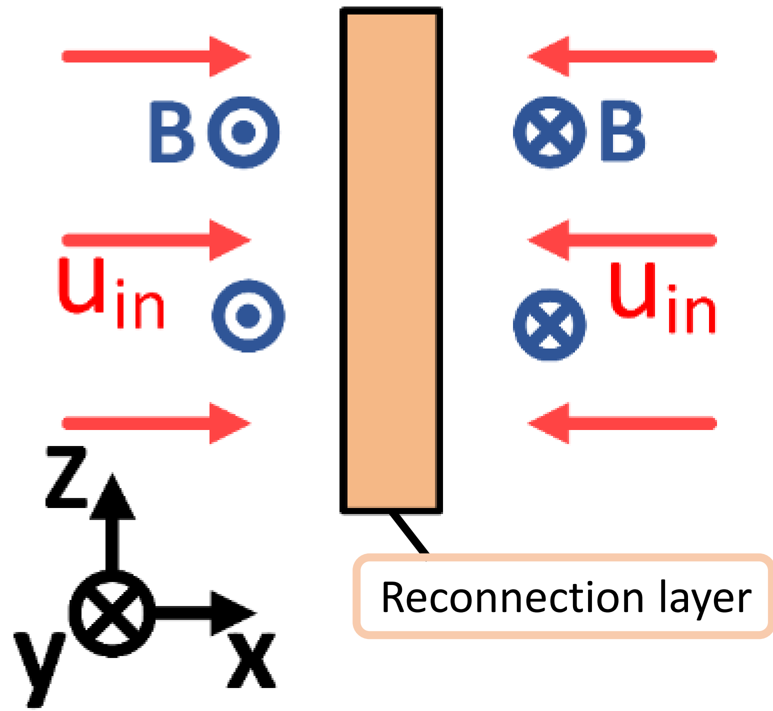

Interferometry ($\mathbf{n_e L}$)

Faraday Rotation Imaging ($\mathbf{B_y}$)

Time Integrated Pinhole Imaging

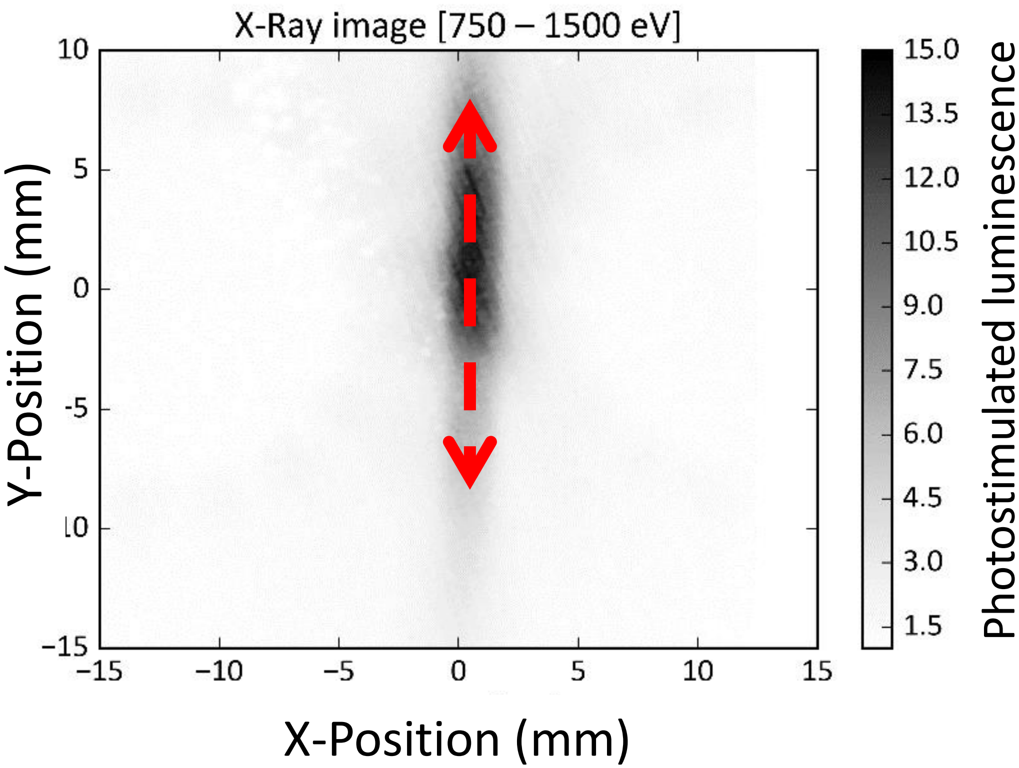

Intensity Profile

$[\ X = 0.0 \pm 2.5 \text{ mm }]$

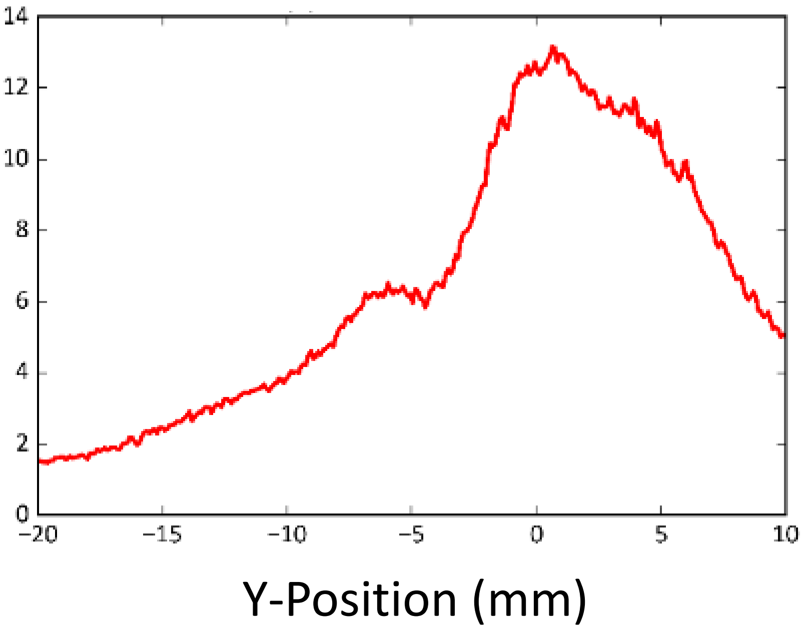

Time Integrated Pinhole Imaging

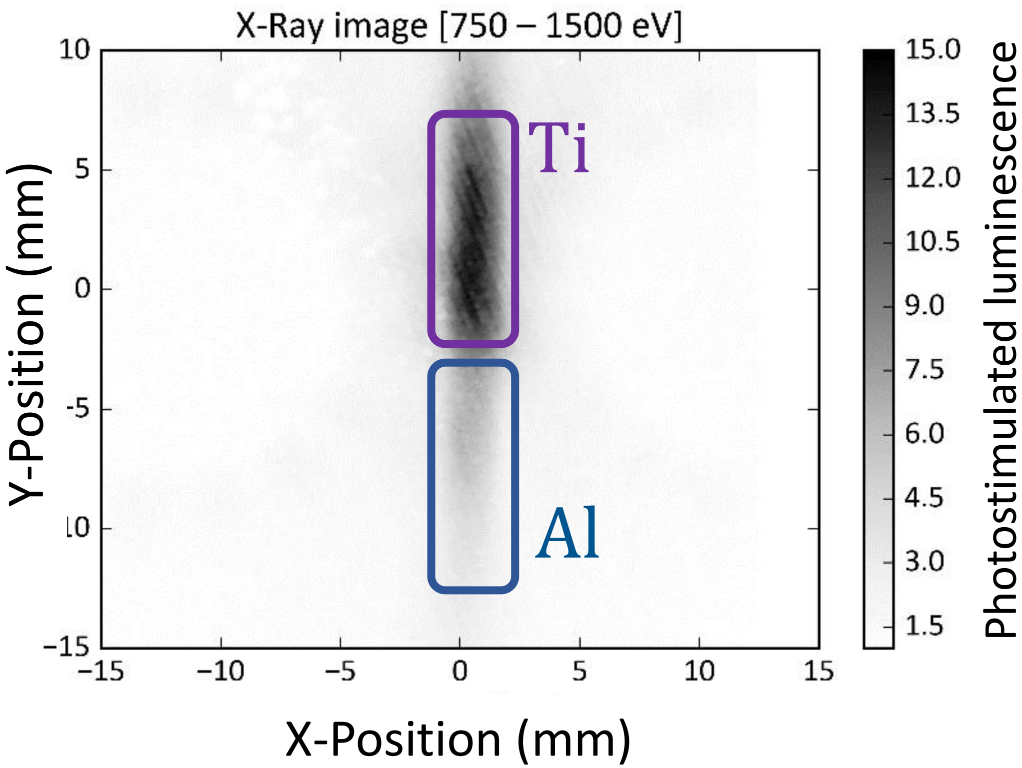

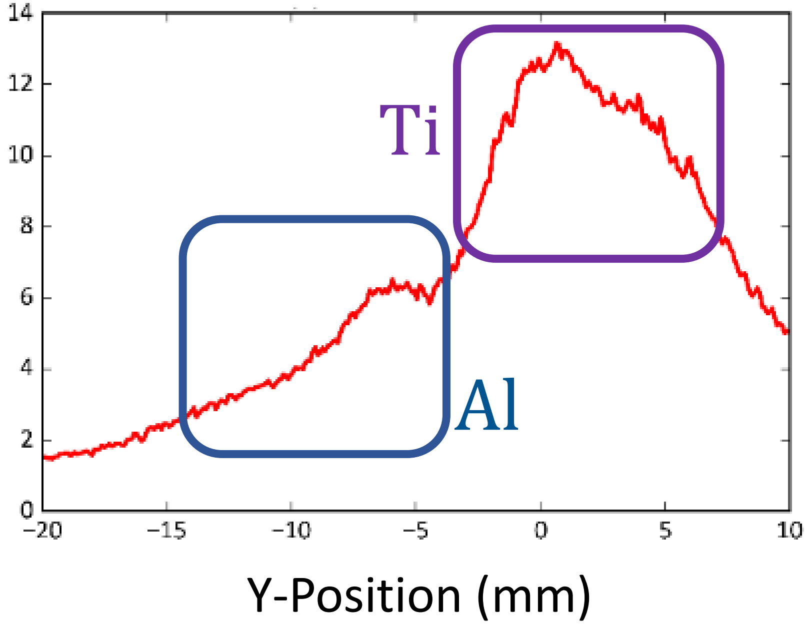

Polypropylene filter transition

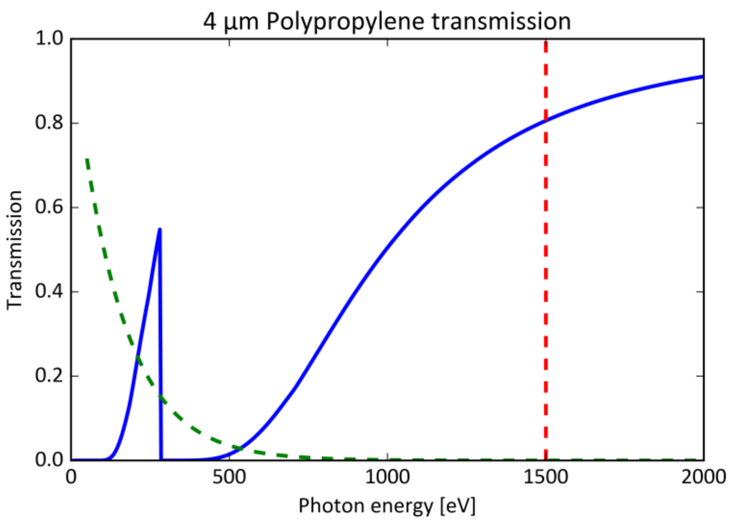

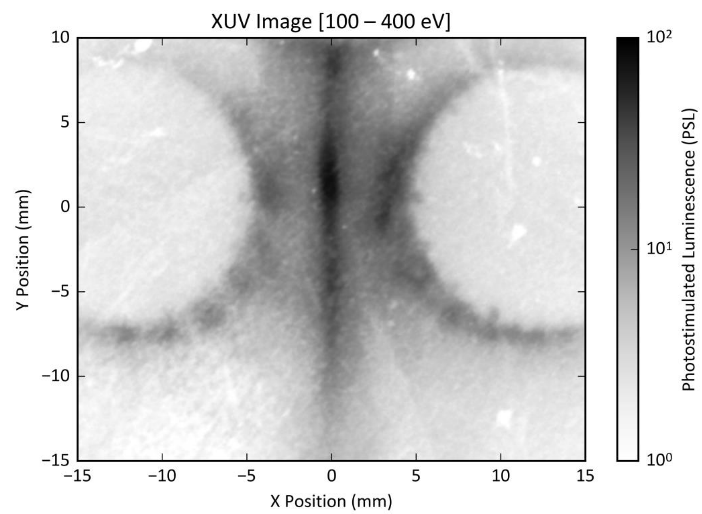

jack.halliday12@imperial.ac.uk

Aluminium filter transition

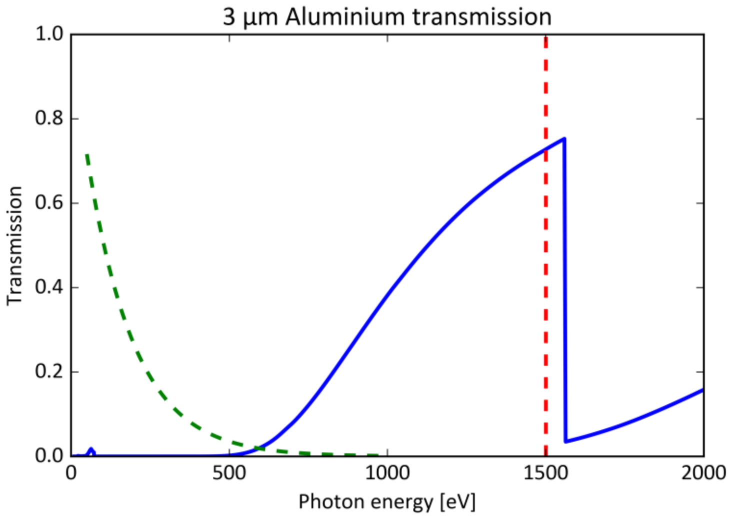

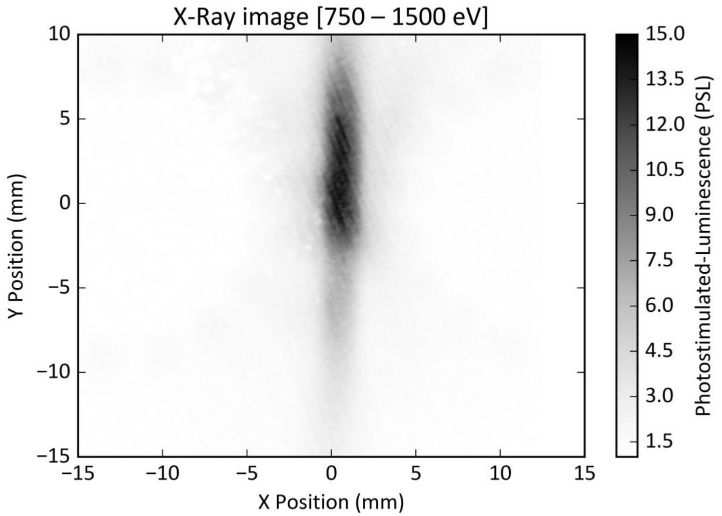

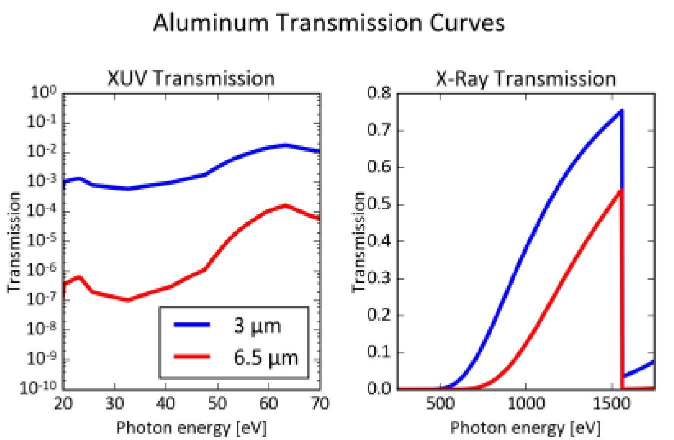

Figure 4.8: Comparison of the transmission spectra of aluminium foils with thicknesses of 6.5 µm and 3 µm, for XUV and X-Ray energies.

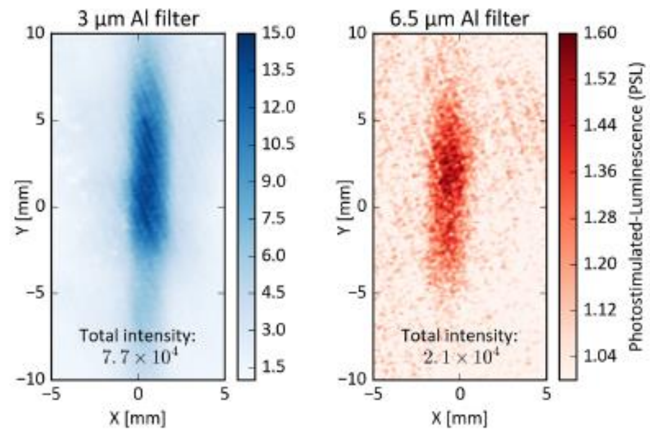

Figure 4.9: End on pinhole images obtained in the same shot (s1016_17) using 800 µm pinholes and two different filters (*blue*- 3 µm aluminium; *red*- 6.5 µm aluminium).

Magnetic Field Profile (Faraday Rotation Imaging)

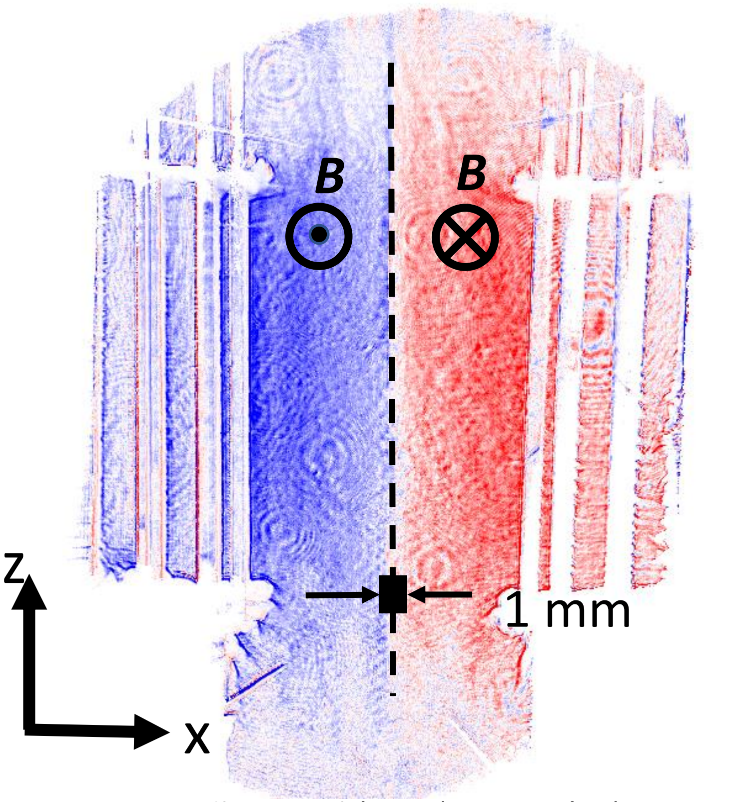

G. F. Swadling et al.(2014). RSI **85** (11), 11E502

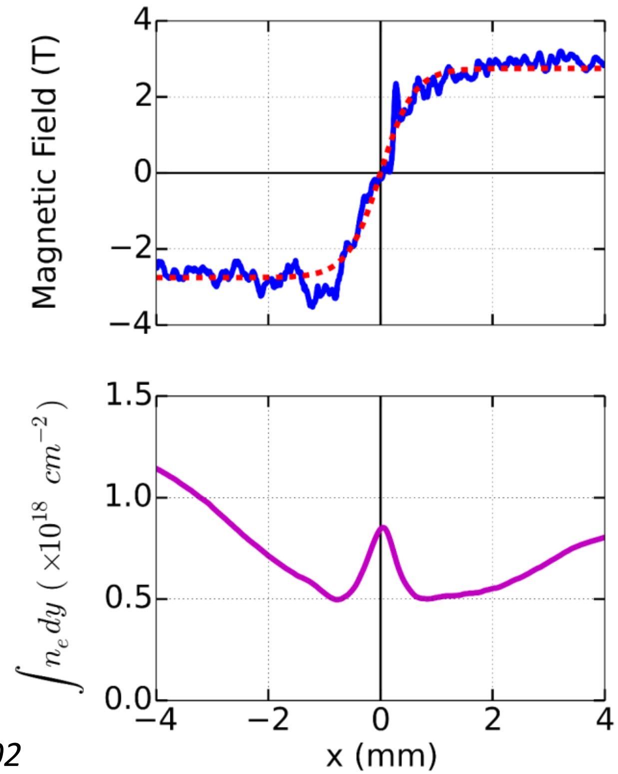

$$\alpha(y,z) \propto \int n_e \boldsymbol{B}.\, d\boldsymbol{x}$$

Harris Sheet:

$$B = B_0 \tanh(x/\delta)$$

$$B_0 = 3\,\mathrm{T}$$

$$\delta = 0.6\,\mathrm{mm}$$

Velocity and Temperature (Thomson Scattering)

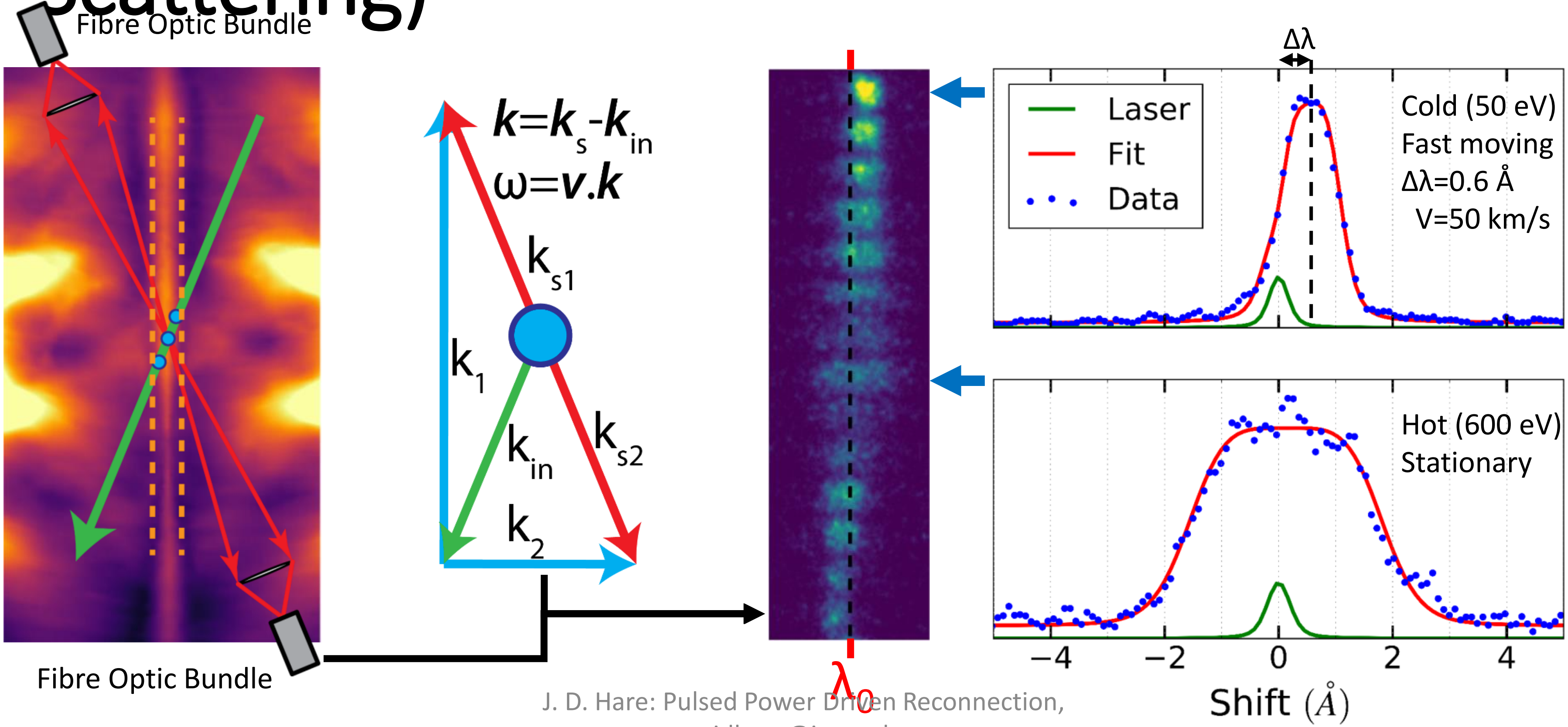

Post-shot images of target

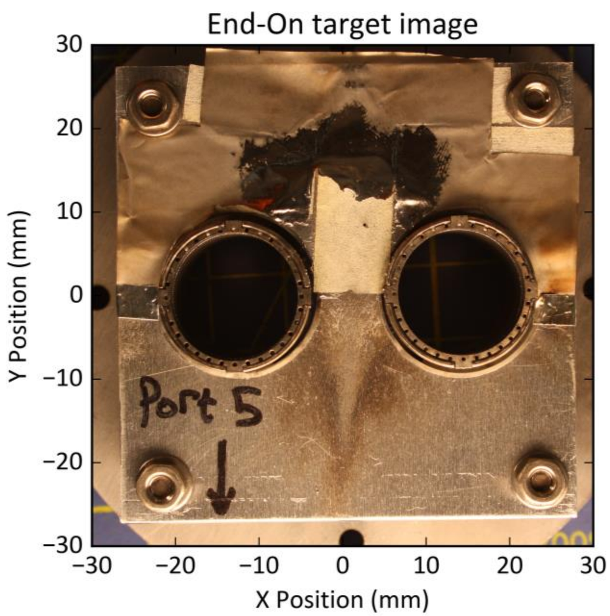

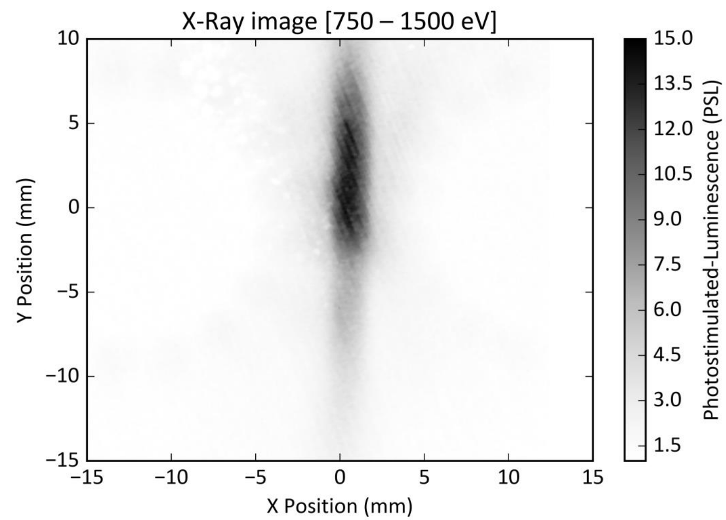

Ionisation cross section

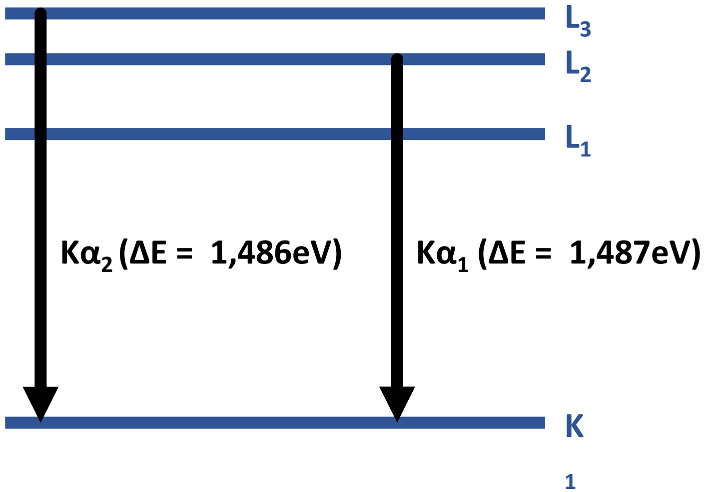

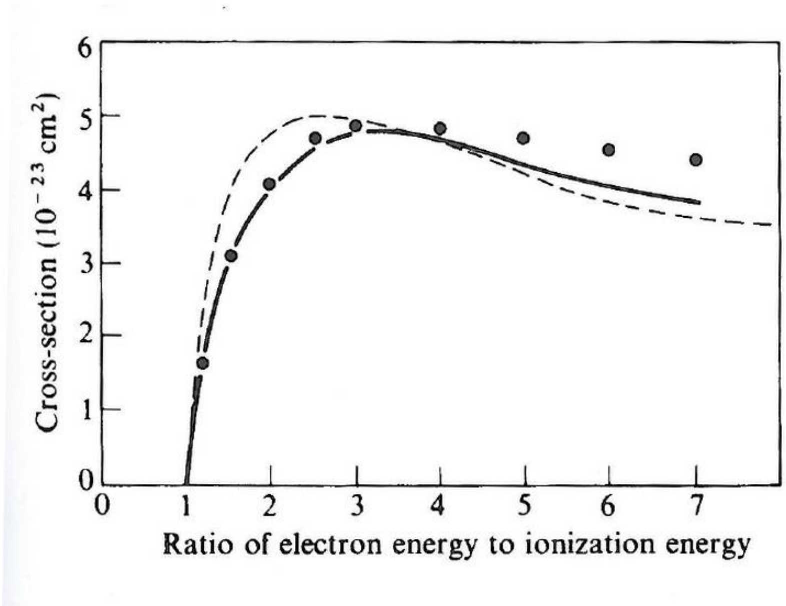

Ref: Dyson, N. A. (2009) X-Rays in atomic and nuclear physics